Dispersion of Droplet Clouds in Turbulence

Humberto Bocanegra Evans,[1] Nico Dam,[2] Guus Bertens,[1] Dennis van der Voort,[1] and Willem van de Water[1,*]
[1]Physics Department, Eindhoven University of Technology, P.O. Box 513, 5600 MB Eindhoven, The Netherlands
[2]Mechanical Engineering Department, Eindhoven University of Technology, P.O. Box 513, 5600 MB Eindhoven, The Netherlands
(Received 23 June 2015; published 14 October 2016)

We measure the absolute dispersion of clouds of monodisperse, phosphorescent droplets in turbulent air by means of high-speed image-intensified video recordings. Laser excitation allows the initial preparation of well-defined, pencil-shaped luminous droplet clouds in a completely nonintrusive way. We find that the dispersion of the clouds is faster than the dispersion of fluid elements. We speculate that preferential concentration of inertial droplet clouds is responsible for the enhanced dispersion.

DOI: 10.1103/PhysRevLett.117.164501

A turbulent flow mixes added contaminants perfectly, but only if these faithfully follow the flow. Particles with inertia lag behind the most rapid velocity changes of the fluid. They are expelled from regions of vorticity and attracted by regions of strain, which results in spontaneous fluctuations of the added particle concentration at the smallest time and length scales of turbulence. This phenomenon is called preferential concentration [1,2] and signifies the tendency of turbulence to *unmix* added matter that has inertia. This remarkable phenomenon, which has been observed both in numerical simulations [3] and experiments [4–10], is of great practical interest for many applications, such as the dispersion of sprays in combustion, the spreading of pollutants in the atmosphere, and the initiation of rain in warm turbulent clouds [11,12].

We use a new experimental technique to study the dynamics of turbulent dispersion of droplets at the smallest length and time scales. Using phosphorescent droplets that can be made to glow by illuminating them with a UV laser, we can delineate a small volume inside a turbulent cloud of droplets and study the evolution of this volume in time. In this Letter, we focus on the evolution of the width of a pencil-shaped cloud, which offers a unique way to study the dispersion of an initially well-delimited cloud of droplets. At initial time, the width of the tagged cloud is 10η, with η the Kolmogorov length scale, the smallest length scale in turbulence.

The motion of inertial particles is a filtered version of the motion of the fluid which carries them. The droplet inertia is quantified by the Stokes number $\mathrm{St} = \tau_p/\tau_\eta$, where τ_η is the turnover time of the smallest eddies in turbulence, the Kolmogorov time, and where the droplet response time τ_p is determined by Stokes friction $\tau_p = \rho_p d_p^2/(18\mu)$, with d_p the droplet diameter, ρ_p the liquid mass density, and μ the dynamic viscosity of air. Filtering of velocity fluctuations is expressed by the formula $v_p/v = (\tau_p/T_f + 1)^{-1/2}$, with v the mean fluctuation fluid velocity and T_f a typical time scale of the flow [13]. For our experiment, this predicts that the largest droplets are approximately 1% slower than air parcels [14].

It is well known, both from experiment and numerical simulations, that, paradoxically, the *relative* dispersion of two droplets, that is, the growth of the distance between them, is *faster* than that of two fluid parcels [17,18]. The question is whether the same holds for the *absolute* dispersion, where a small puff of droplets is released from a point or a line and is subsequently dispersed by turbulence as time progresses.

The relative dispersion of two point particles has been measured in an experiment involving a swirling turbulent flow [18] (a von Kármán flow between rotating disks). It was found that, on average, the distance between two inertial particles increases faster than the separation of two fluid parcels. The same phenomenon was found in numerical simulations, the enhancement of relative dispersion being largest when the droplets start close together, with the initial separation comparable to the Kolmogorov scale η [17]. The occurrence of caustics [11,19,20] is thought to be responsible for the enhanced particle dispersion.

In an experiment, the relative dispersion of particle pairs is normally measured by tracking many particles simultaneously and computing the change of their mutual distances. In this way, a measurement of the evolution of the particle distribution inside a dense cloud would be very difficult. Similarly, it would require a special numerical simulation in which the evolution of a small dense cloud with initial size comparable to the Kolmogorov length is followed. These simulations have not yet been performed.

Optical selection of an initial particle distribution makes an ideal experiment to study particle dispersion. The selection is not intrusive, while the droplets have already adapted to the turbulence. These conditions are naturally realized in our experiments, where we tag a volume of droplets by making them glow. In experiments where a cloud of droplets is injected, it is difficult to avoid perturbation of the flow and make the droplets forget their initial condition.

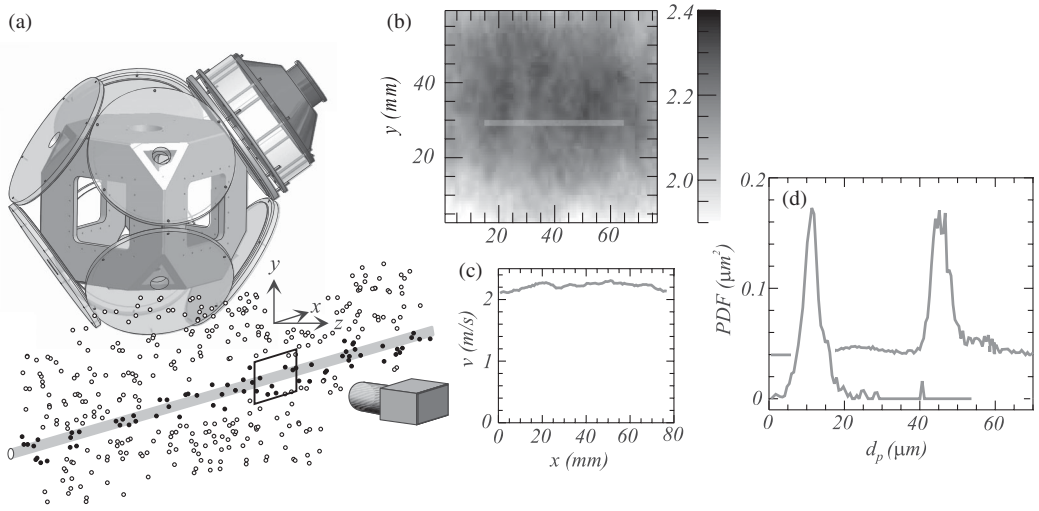

FIG. 1. (a) Experimental setup, not to scale. It consists of a closed chamber in which turbulence is generated by loudspeaker-driven synthetic jets. For clarity, only one loudspeaker is shown. The chamber contains a fog of approximately monodisperse droplets which are made from a water-based phosphorescent solution. A pencil-shaped volume is delineated by exciting phosphorescence with a pulsed focused laser beam. The glowing droplets are followed using a fast intensified camera. (b) Uniformity of the turbulent velocity v (vertical y component) inside the chamber. The initially delineated pencil-shaped volume which is imaged by the camera (50.1 mm long) is indicated. (c) Turbulent velocity v along the delineated pencil. (d) Volume-weighted droplet size probability distribution function (PDF) for two rotation rates of the spinning disk, corresponding to mean droplet diameters of $d_p = 12$ μm and $d_p = 46$ μm, respectively. These PDFs are normalized; the PDF of the 46 μm droplets has been shifted vertically for clarity.

We have measured the dispersion of thin pencil-shaped clouds by exciting droplets using a weakly focused beam of a pulsed UV laser [see Fig. 1(a)]. Let us call $t = 0$ the instant where the cloud was delineated optically. The cloud evolves in time as it is deformed and advected by the turbulent flow. We trace the glowing droplets at a frame rate of 10 kHz using a high-speed camera (Photron SA-Z) with a gated image intensifier (Lambert Instruments, HICAM 5000). Each pencil-shaped cloud was followed during 1.2 ms, which is comparable to the lifetime of the phosphorescence. This experiment is repeated at each laser shot, and the images are phase averaged. In this manner, the growing size of the averaged cloud with increasing time reflects *absolute* turbulent dispersion. The prime quantity is the averaged transverse luminosity profile $I(y,t)$ of the cloud. It was measured by collapsing the pencil-shaped clouds along the x axis, while the camera already integrates the intensity along the line of sight (z axis). The intensity $I(y,t)$ is all that is needed to measure absolute dispersion at small length and time scales.

In view of the Gaussian character of the fluctuating air velocity, we quantify the dispersion by assuming that a unit pointlike concentration released in the origin spreads isotropically as $I(r,t) = \sigma(t)^{-3}\pi^{-3/2}\exp[-r^2/\sigma(t)^2]$. Consequently, an initial concentration profile $I_0(y)$ as observed from our phase-averaged images would evolve as

$$I(y,t) = \frac{1}{\pi^{1/2}\sigma(t)}\int_{-\infty}^{\infty} I_0(y')e^{-[y-y'-y_0(t)]^2/\sigma(t)^2}dy', \quad (1)$$

where $y_0(t)$ allows for a droplet motion due to a residual mean velocity in the chamber.

In principle, the full three-dimensional initial tagged droplet distribution $I_0(y,z)$ would be needed, followed by its projection on the camera image plane at later times. However, the Gaussian assumption, which of course must be verified in the experiment, only needs the projection of $I_0(y)$. If the (projected) initial distribution were Gaussian, $I_0(y) = \pi^{-1/2}\sigma_0^{-1}\exp(-y^2/\sigma_0^2)$ with initial Gaussian width σ_0, $\langle(y(t)-y_0)^2\rangle = [\sigma_0^2 + \sigma(t)^2]/2$. However, in our experiment the intensity profile of the laser beam is not smooth (we use a multimode frequency-tripled Nd:YAG laser), while the excitation of phosphorescence depends nonlinearly on the laser intensity. This, in general, does not lead to an initial Gaussian intensity profile, and the more general description of Eq. (1) must be used instead.

In the experiment, the fate of small clouds (diameter $\approx 10\eta$) of St ≈ 1 droplets can be followed in a turbulent flow with large Reynolds number, large enough to clearly separate the stirring and viscous length scales, so that the observed phenomena do not depend on the way turbulence is generated. A schematic drawing of the experiment is shown in Fig. 1(a). Strong turbulence, reaching Taylor-based Reynolds numbers $\mathrm{Re}_\lambda \approx 460$, is generated inside a closed chamber. The chamber has a similar design to that described by Hwang and Eaton [21], using eight loudspeaker-driven synthetic jets to stir the air inside the chamber while maintaining near-zero average flow. The cubical chamber has a side length of 0.4 m, while the images cover a region of interest with size 51×51 mm^2

in the center of the chamber (resolution 60 μm per pixel). In this region of interest, the turbulence, whose characteristics were measured in a separate experiment using particle image velocimetry is isotropic and approximately homogeneous. Reaching (approximate) homogeneity in this flow required meticulous balancing of the loudspeaker drive currents. The latter consisted of colored noise, summed to 0 so that pressure variations inside the chamber were minimized. The homogeneity of the vertical component of the turbulent velocity is shown in Fig. 1(b); it varies by approximately 10% over the initially delineated volume. The corresponding residual mean velocity is ≈ 0.2 m/s. The measured longitudinal correlation function can be approximated by $C(r) \propto \exp(-r/L)$ with $L \approx 70$ mm, so that the integral scale L exceeds our measurement volume.

Particle image velocimetry provides velocity information averaged over square windows with size 20η, and a special procedure is needed to infer the small-scale characteristics of the turbulence [22]. The typical turbulent velocity is $v = 2.15$ m/s, and the turbulent dissipation rate is $\epsilon = 90\ \mathrm{m^2\,s^{-3}}$, from which follow the Taylor-based Reynolds number $\mathrm{Re}_\lambda = 490$, the Kolmogorov length scale $\eta = 7.8 \times 10^{-5}$ m, and the Kolmogorov time scale $\tau_\eta = 4.1 \times 10^{-4}$ s.

We use a spinning-disk aerosol generator to produce relatively monodisperse droplets and measure the droplet diameter using interferometric particle imaging [23]. In our experiment, we scan the Stokes number by tuning the droplet size through the rotation rate of the spinning-disk droplet generator. The luminescence intensity of the glowing droplets is proportional to their volume, and a volume-weighted size distribution is shown in Fig. 1(d). It is a challenge to produce monodisperse droplets in the large quantities needed for this experiment, but we are aided by the phosphorescence technique which effectively narrows their size distribution. The width of the particle-size distribution leads to a relatively large uncertainty in the Stokes number St, as St is proportional to the square of the droplet diameter. The largest droplet diameter (50 μm) in these experiments is still smaller than the Kolmogorov length ($\eta = 78$ μm).

Our droplets are small and move in strong turbulence. Therefore, the influence of gravity is expected to be negligible. Gravity can be quantified by a terminal sinking velocity v_T which is a small fraction of the turbulent velocity. For the largest drops, $v_T/v = (4 \pm 1) \times 10^{-2}$, while for the smallest drops, $v_T/v = (4 \pm 3) \times 10^{-3}$, and where the variation is determined by the width of the droplet size PDF [see Fig. 1(d)].

The phosphorescent droplet tagging technique was inspired by [24]. The droplets are formed from a phosphorescent water-based solution which has been doped with europium-(III)-chloride hexahydrate and uses thenoyltrifluoroacetone (TTA) and trioctylphosphine oxide (TOPO) as ligands. The concentrations of the different ingredients are 8.3×10^{-5} M Eu^{3+}, 8.3×10^{-4} M TTA, 8.3×10^{-4} M TOPO [25]. The solution has a phosphorescence decay constant of ≈ 600 μs, an excitation wavelength of 355 nm, and an emission wavelength of 613 nm. The illumination with UV light easily saturates the excitation. Therefore, the laser beam profile must be shaped judiciously in order to excite a narrow pencil-like volume. In fact, saturation and scattering of light is responsible for the broad tails of the initial profile in Fig. 2(b).

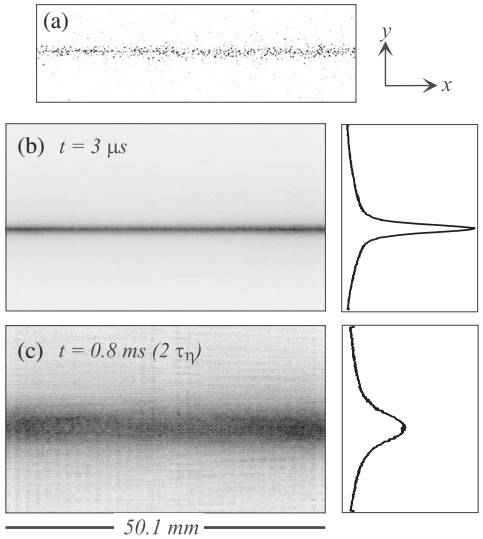

FIG. 2. Dispersion of pencil-shaped volumes delineated at $t = 0$ in a turbulent cloud. (a) Single tagged volume at initial time. (b) Initially tagged volume, averaged over 775 cycles. (c) Tagged volume after $t = 0.8$ ms (corresponding to $t = 2\tau_\eta$). The cross-sectional intensity profiles of the phase-averaged images are indicated.

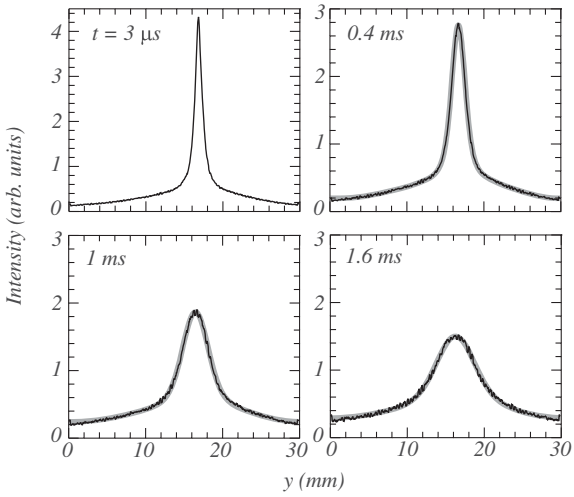

FIG. 3. Cross-sectional profiles of tagged volume at initial time ($t = 3$ μs) and after $t = 0.4$, 1.0, and 1.6 ms after tagging. The initial profile is used in Eq. (1) for a fit of the widening $\sigma(t)$. The fits are indicated by the thick gray lines.

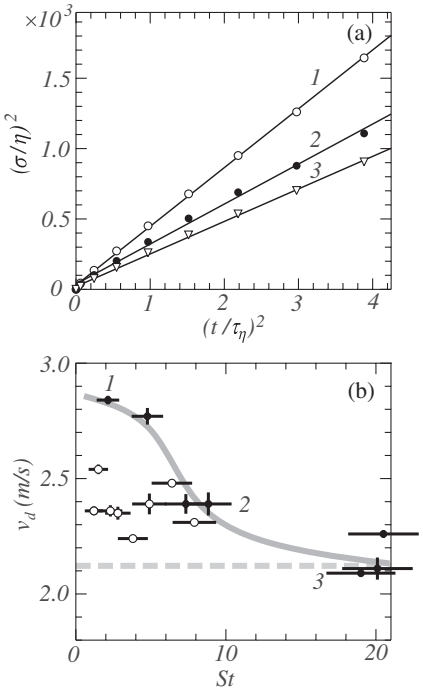

FIG. 4. Line dispersion as a function of Stokes number. (a) Time dependence of linewidth $\sigma(t)$ for three different Stokes numbers $\mathrm{St} = 2.1$, 8.8, and 20 for the lines labeled by 1, 2, and 3, respectively. The symbols are the measurements, the full lines are fits, and $\sigma^2(t) = 2v_d^2t^2$, with v_d the dispersion velocity. (b) Closed dots represent the dispersion velocity of narrow lines, starting with an initial Gaussian width $\sigma_0 = 10\eta$; open circles correspond to $\sigma_0 = 30\eta$. The horizontal error bars were computed from the width of the volume-weighted droplet diameter PDF [see Fig. 1(d)]; the vertical error bars were computed using a decimation procedure. Where the vertical error bars are absent, no decimation of the data was possible. The thick dashed line is the turbulent velocity v, and the thick solid line is to guide the eye to the results with the narrowest initial cloud. The numbered data points correspond to the numbered lines in (a).

The dispersion experiments consist of tagging a thin pencil-like volume with diameter $\sigma_0 = 10\eta$ at the center of the turbulent cloud and recording its evolution in time. Every tagging realization (a cycle) results in a recording of 12 frames. For every case, we collect 775 sequences. The data are then phase averaged over cycles, and a mean intensity profile is obtained for each time step by summing the distribution horizontally. For two delay times, the result is shown in Fig. 2.

Next, this intensity profile is fitted using Eq. (1), taking for the initial profile $I_0(y)$ the measurement 3 μs after tagging. (The small delay is introduced to avoid capturing elastically scattered laser light and fluorescence.) This procedure, illustrated in Fig. 3, produces perfect fits. The result is the time-dependent Gaussian width $\sigma(t)$, which for a typical experiment is plotted in Fig. 4(a). The width can be fitted well using $\sigma^2(t) = 2v_d^2t^2$, with v_d the droplet dispersion velocity. It should be compared to the dispersion velocity of air parcels, which for short times equals the turbulent velocity v.

The statistical error in the dispersion velocities was estimated by dividing the total number of sequences in 10 blocks and computing a dispersion velocity for each of them. The variance of the found velocities was taken as the statistical error. The uncertainty in the Stokes number was computed from the width of the volume-weighted droplet diameter PDF (see Fig. 1).

Our main result is shown in Fig. 4(b). We find that small clouds of droplets spread faster than fluid parcels, that is, $v_d > v$. Figure 4(b) shows the results for pencils with two different initial Gaussian widths $\sigma_0/\eta = 10$ and 30, respectively. In both cases, their dispersion velocity exceeds the turbulent air velocity at $\mathrm{St} \lesssim 20$, but at small Stokes numbers $\mathrm{St} = \mathcal{O}(1)$, the narrowest initial cloud spreads fastest.

Although the enhanced relative dispersion of inertial droplets is well known [17,18], our results are unexpected as they are about *absolute* dispersion. The emergence of a length scale $\approx 10\eta$ suggests a connection with preferential concentration.

In conclusion, we have exploited a technique to make small clouds of droplets glow inside a strongly turbulent flow and find that for short times and small length scales these clouds disperse faster than genuine fluid tracers. This is a new nonintrusive way to instantaneously create Lagrangian distributions of many droplets that are already immersed in a turbulent flow.

This work is part of the research program of the "Stichting voor Fundamenteel Onderzoek der Materie (FOM)," which is financially supported by the "Nederlandse Organisatie voor Wetenschappelijk Onderzoek (NWO)." This work is also supported by the COST Action MP0806.

*w.v.d.water@tue.nl

[1] M. Maxey, J. Fluid Mech. **174**, 441 (1987).
[2] K. D. Squires and J. K. Eaton, Phys. Fluids A **3**, 1169 (1991).
[3] J. Bec, L. Biferale, M. Cencini, A. Lanotte, S. Musacchio, and F. Toschi, Phys. Rev. Lett. **98**, 084502 (2007).
[4] J. R. Fessler, J. D. Kullick, and J. K. Eaton, Phys. Fluids **6**, 3742 (1994).
[5] A. M. Wood, W. Hwang, and J. K. Eaton, Int. J. Multiphase Flow **31**, 1220 (2005).
[6] J. P. L. Salazar, J. de Jong, L. Cao, L. Woodward, H. Meng, and L. R. Collins, J. Fluid Mech. **600**, 245 (2008).
[7] E. Saw, R. Shaw, S. Ayyalasomayajula, P. Chuang, and A. Gylfason, Phys. Rev. Lett. **100**, 214501 (2008).
[8] S. Balachandar and J. K. Eaton, Annu. Rev. Fluid Mech. **42**, 111 (2010).
[9] R. Monchaux, M. Bourgoin, and A. Cartellier, Phys. Fluids **22**, 103304 (2010).

[10] L. Fiabane, R. Zimmermann, R. Volk, J.-F. Pinton, and M. Bourgoin, Phys. Rev. E **86**, 035301 (2012).
[11] G. Falkovich, A. Fouxon, and M. Stepanov, Nature (London) **419**, 151 (2002).
[12] W. W. Grabowski and L.-P. Wang, Annu. Rev. Fluid Mech. **45**, 293 (2013).
[13] L.-P. Wang and D. E. Stock, J. Atmos. Sci. **50**, 1897 (1993).
[14] The prediction of a smaller particle velocity $v_p/v < 1$ is not without controversy. In a numerical simulation, Salazar and Collins [15] show that very small $\mathrm{St} \approx 0.2$ droplets have a 2% larger velocity than the turbulent air. For larger Stokes numbers, the prediction of Wang and Stock [13] has recently been verified in numerical simulations and experiments by Good *et al.* [16].
[15] J. P. L. C. Salazar and L. C. Collins, J. Fluid Mech. **696**, 45 (2012).
[16] G. H. Good, P. J. Ireland, G. P. Bewley, E. Bodenschatz, L. R. Collins, and Z. Warhaft, J. Fluid Mech. **759**, R3 (2014).
[17] J. Bec, L. Biferale, A. Lanotte, A. Scagliarini, and F. Toschi, J. Fluid Mech. **645**, 497 (2010).
[18] M. Gibert, H. Xu, and E. Bodenschatz, Europhys. Lett. **90**, 64005 (2010).
[19] M. Wilkinson and B. Mehlig, Europhys. Lett. **71**, 186 (2005).
[20] G. P. Bewley, E. Saw, and E. Bodenschatz, New J. Phys. **15**, 083051 (2013).
[21] W. Hwang and J. K. Eaton, Exp. Fluids **36**, 444 (2004).
[22] G. Bertens, D. van der Voort, and W. van de Water, Exp. Fluids **56**, 89 (2015).
[23] H. Bocanegra Evans, N. Dam, D. van der Voort, G. Bertens, and W. van de Water, Rev. Sci. Instrum. **86**, 023709 (2015).
[24] S. Krüger and G. Grünefeld, Appl. Phys. B **71**, 611 (2000).
[25] N. Arnaud and J. Georges, Spectrochim. Acta, Part A **59**, 1829 (2003).